

Apoptosis of Sertoli cells after conditional ablation of murine double minute 2 (Mdm2) gene is p53-dependent and results in male sterility

S Fouchécourt^{*,1,2,3,4,9}, G Livera^{5,9}, S Messiaen⁵, B Fumel^{1,2,3,4}, A-S Parent⁶, J-C Marine^{7,8} and P Monget^{1,2,3,4}

Beside its well-documented role in carcinogenesis, the function of p53 family has been more recently revealed in development and female reproduction, but it is still poorly documented in male reproduction. We specifically tested this possibility by ablating *Mdm2*, an E3 ligase that regulates p53 protein stability and transactivation function, specifically in Sertoli cells (SCs) using the AMH-Cre line and created the new SC-*Mdm2*^{-/-} line. Heterozygous SC-*Mdm2*^{-/+} adult males were fertile, but SC-*Mdm2*^{-/-} males were infertile and exhibited: a shorter ano-genital distance, an extra duct along the vas deferens that presents a uterus-like morphology, degenerated testes with no organized seminiferous tubules and a complete loss of differentiated germ cells. In adults, testosterone levels as well as StAR, P450c17 (*Cyp17a1*) and P450scc (*Cyp11a1*) mRNA levels decreased significantly, and both plasma LH and FSH levels increased. A detailed investigation of testicular development indicated that the phenotype arose during fetal life, with SC-*Mdm2*^{-/-} testes being much smaller at birth. Interestingly, Leydig cells remained present until adulthood and fetal germ cells abnormally initiated meiosis. Inactivation of *Mdm2* in SCs triggered p53 activation and apoptosis as early as 15.5 days post conception with significant increase in apoptotic SCs. Importantly, testis development occurred normally in SC-*Mdm2*^{-/-} lacking p53 mice (SC-*Mdm2*^{-/-}p53^{-/-}) and accordingly, these mice were fertile indicating that the aforementioned phenotypes are entirely p53-dependent. These data not only highlight the importance of keeping p53 in check for proper testicular development and male fertility but also certify the critical role of SCs in the maintenance of meiotic repression.

Cell Death and Differentiation (2016) 23, 521–530; doi:10.1038/cdd.2015.120; published online 16 October 2015

Sertoli cells (SCs) are the supporting cell lineage of the male germ line and their function is critical for male fertility. SCs differentiate early during fetal life; they are the first cells that differentiate in the testes and they drive the sexual differentiation of the gonad (for review, see Svigen and Koopman¹). In the mouse, these cells start forming cords by enclosing germ cells as early as 12 days post conception. SCs are responsible for providing germ cells with a specialized environment to promote their survival and orchestrate their differentiation throughout life. They also allow the differentiation of Leydig cells through paracrine signaling, including Desert hedgehog signaling, for example,² and promote their activity.³ SCs are involved in masculinizing the embryo as they produce high levels of anti-Müllerian hormone (AMH) that triggers the regression of the future female genitalia. Strikingly, SCs only proliferate during fetal and post-natal life, and definitively cease cycling around 10 days postpartum. Interestingly, these cells are relatively resistant to apoptosis in response to DNA damage. It has been proven in developing rat testes that these cells easily survive a high dose of radiation exposure.⁴ The

mechanisms underlying the poor responsiveness of SCs to DNA damage remains elusive. In the human embryonic testis, the mild apoptotic response of SCs following radiation is decreased by pharmacological inhibition of p53 with pifithrin alpha.⁵

The role of p53 has been largely documented as the ‘guardian of the genome’; owing to its deregulation in numerous cancers, it is considered as a major tumor suppressor. From a model organism, it appears that p53 homologs are also key regulators of development and reproduction. Interestingly in mammals, p53-related proteins (i.e., p63 or p73) are also involved in the development of the central nervous system. Inactivation of any of the three p53 family members impairs mouse female fertility.^{6,7} On the other hand, the data relating p53 to male fertility are still scarce. So far, in testis, the function of p53 is little documented, except in testicular germ cell tumors⁸ and germ cell apoptosis (apoptosis of prenatal sperm cells⁹ and of damaged sperm in the adult¹⁰). The *murine double minute 2* gene *Mdm2* belongs to a large family of RING finger-containing proteins,

¹INRA, UMR85 Physiologie de la Reproduction et des Comportements, F-37380 Nouzilly, France; ²CNRS, UMR6175 Physiologie de la Reproduction et des Comportements, F-37380 Nouzilly, France; ³Université François Rabelais de Tours, F-37041 Tours, France; ⁴IFCE, F-37380 Nouzilly, France; ⁵Laboratoire de Développement des Gonades, INSERM U967, CEA/DSV/iRCM/SCSR/LDG, Univ Paris Diderot, Sorbonne Paris Cité, F-92265 Fontenay-Aux-Roses, France; ⁶Developmental Neuroendocrinology Unit, GIGA Neurosciences, University of Liège, CHU Sart Tilman, Liège, Belgium; ⁷Laboratory for Molecular Cancer Biology, Center for Human Genetics, KU Leuven, Leuven, Belgium and ⁸Center for the Biology of Disease, VIB, Leuven, Belgium

*Corresponding author: S Fouchécourt, INRA, UMR85 Physiologie de la Reproduction et des Comportements, F-37380 Nouzilly, France. Tel: +33 (0) 247 427 271; Fax: +33 (0) 247 427 743; E-mail: sophie.fouchecourt@tours.inra.fr

⁹These authors contributed equally in this work.

Abbreviations: SCs, Sertoli cells; *Mdm2*, Murine double minute 2; AGD, Ano-genital distance; *En*, embryonic age *n*; *Pn*, post-natal age *n*

Received 19.12.14; revised 03.7.15; accepted 31.7.15; Edited by M Oren; published online 16.10.15

and functions mainly as an E3 ligase regulating the activity of various substrates by ubiquitylation (mono- or poly- ubiquitylation). Among the substrates is the p53 tumor suppressor, which is responsible for transcriptional activation of genes involved in the cell cycle, apoptosis and cell aging.^{11–13} Overexpression of Mdm2 is one of the mechanisms that leads to p53 inactivation by promoting its proteasome-dependent degradation after ubiquitylation in the tumors that retain wild-type p53 (for review, see Marine and Lozano¹⁴). In addition, Mdm2 can bind the p53 transactivation domain and directly interfere with p53 transcriptional regulatory mechanisms. Mdm2-null mice are not viable because of early embryonic lethality (E3.5), but are viable in a p53-null background.^{15,16} To test whether the suppression of p53 function is required for testicular development and male fertility, we inactivated specifically *Mdm2* in SCs using the AMH-Cre line.¹⁷

Results

Mdm2 mRNA was detected in testes (adult and P10) and was present in SC-enriched fractions from prepubertal P10 mice (Supplementary data 1). To test the hypothesis of the critical

role of Mdm2 in SCs, we created a transgenic line with targeted inactivation of *Mdm2* specifically in SCs by crossing AMH-Cre and *Mdm2*^{LL} lines, and named this new line SC-Mdm2^{-/-}. The contemporary Cre-Mdm2^{LL} littermate controls were called Cre-. We verified that the allele lacking exons 5 and 6 (*Mdm2*[δ exons5/6]) after the Cre recombination event (226 bp) was detected in testes but not in any other tissues (Supplementary data 2).

At adulthood (3 months), SC-Mdm2^{-/-} males were infertile and had very small testes (Figures 1a–d; testis weight: SC-Mdm2^{-/-} 5.35 mg^{***} \pm 1.40 versus Cre- 112.8 mg \pm 4.5, $P < 0.001$), an abnormal external genital tract and a shorter ano-genital distance compared with Cre- (Figures 1g and h). Conversely, heterozygous SC-Mdm2^{+/-} males were normally fertile and had a normal genital tract (not shown). Testicular histology in adult SC-Mdm2^{-/-} (Figure 2A) was characterized by the absence of seminiferous tubule organization and differentiated germ cells.

Seminal vesicles and epididymides were significantly smaller in SC-Mdm2^{-/-} than in Cre- (seminal vesicle weight: SC-Mdm2^{-/-} 137.7 mg^{***} \pm 22.2 versus Cre- 448.5 mg \pm 30.7, $P < 0.001$; epididymis weight: SC-Mdm2^{-/-} 30.3 mg^{***} \pm 4.84

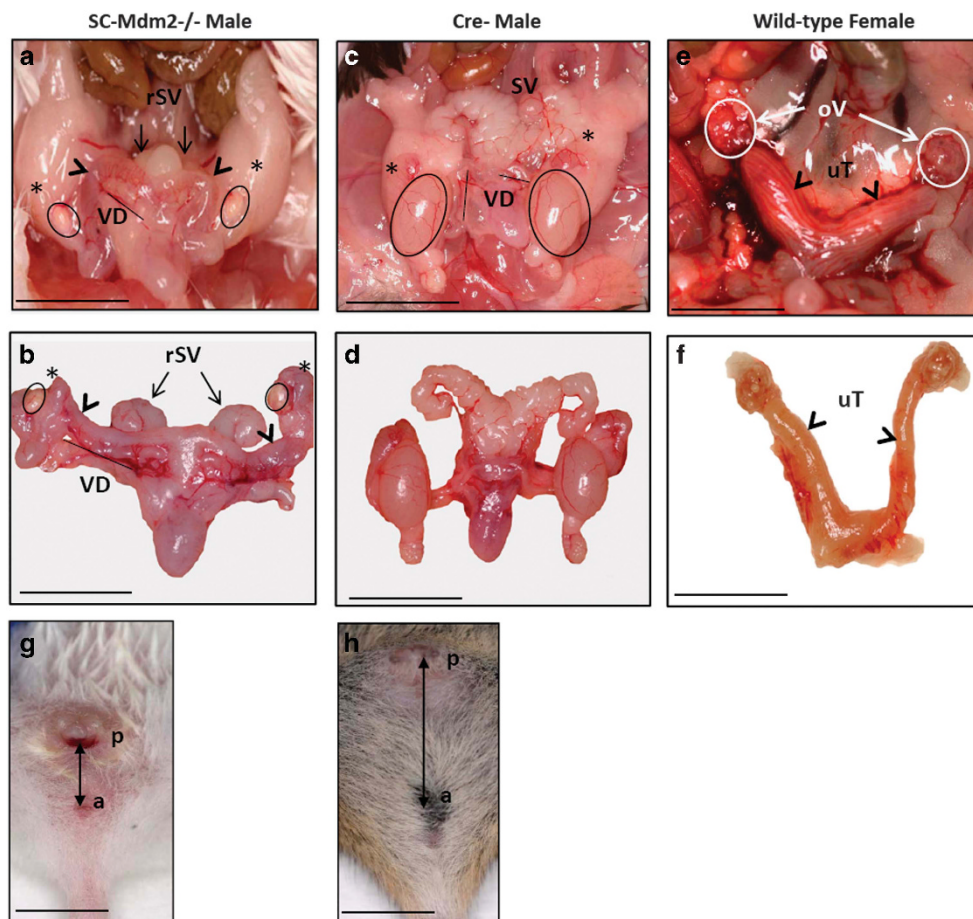


Figure 1 Internal genital tract of SC-Mdm2^{-/-} males (a and b) compared with Cre- (c and d) and normal female tracts (e and f). Black circles are positioned on testes, stars on the caput of the epididymis, and arrowheads on the extra ducts present in SC-Mdm2^{-/-} (a, b) and the uterus in females (e). SV: seminal vesicles; rSV: reduced seminal vesicles; VD: vas deferens. Ov: ovary (E: white circles); uT: uterus. External genital tract of SC-Mdm2^{-/-} males (g/h). Arrows show the AGD in SC-Mdm2^{-/-} (g) and Cre- (h) males. a = anus, p = penis. Bar represents 1 cm

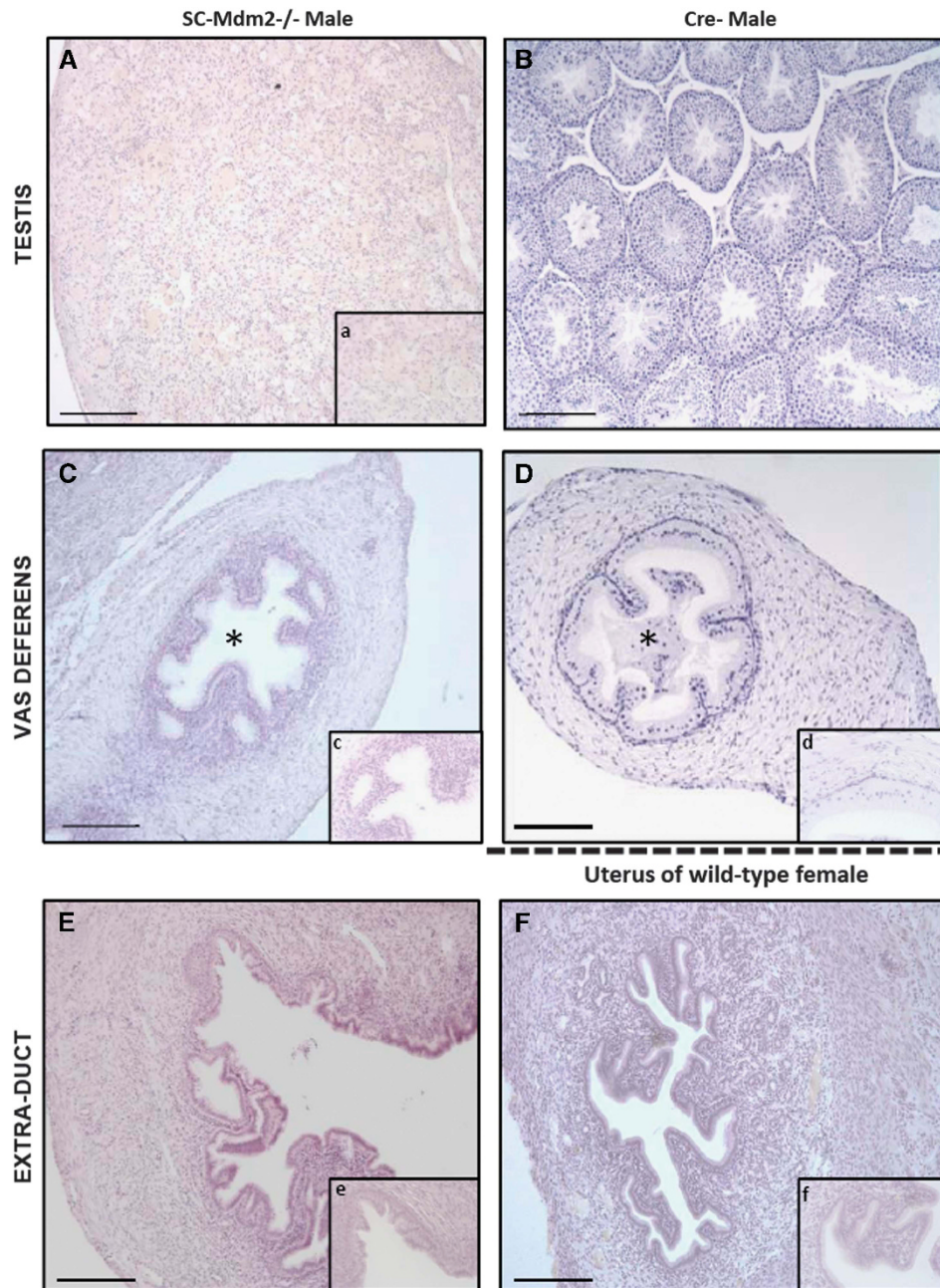


Figure 2 Histology sections (hematoxylin staining) of testes and ducts in adult SC-Mdm2^{-/-} males (A, C, E) compared with Cre- males for testes and vas deferens (B, C) and females for uterus (E, F). Testicular cells were not organized in seminiferous tubules in adult SC-Mdm2^{-/-} testes (A, a) and no differentiated germ cells were present. No sperm was present in the lumen (*) of the vas deferens contrary to Cre- (C, c and D, d). The histology of the extra duct was similar to the uterus (E, e and F, f). Bar in large windows represents 100 μ m; magnification is four times greater in small windows (a, c, d, e, f)

versus Cre- 48.6 mg \pm 2.2, $P < 0.001$) (Figure 1a–d). Interestingly, we observed an extra duct along the vas deferens with the apparent aspect of a uterus (Figures 1a, b, e and f) and histology similar to the uterus (Figures 2E and F); the histology of the vas deferens was normal (Figures 2C and D); no sperm was present in the lumen.

In correlation with a decrease in seminal vesicle weight, plasma testosterone levels significantly decreased in SC-Mdm2^{-/-} (Figures 3a, $n = 8$ for each genotype), along with mRNA levels per testis of Cyp17a1 (P450c17), Cyp11a1

(P450scc) and StAR (Figure 3b, $n = 5$ for each genotype). Consequently, LH levels significantly increased by a factor of around 7 in SC-Mdm2^{-/-} compared with Cre- (Figure 3c; $P < 0.001$). Interestingly, FSH levels also significantly increased in SC-Mdm2^{-/-} (Figure 3d; $P < 0.001$).

As AMH-Cre is expected to induce the deletion of the *Mdm2* allele during fetal life (around E15), we sought to determine the precise kinetics of the appearance of this phenotype. Testes were harvested at various stages during fetal (E15, E16, E18) and post-natal life (P1) (Figures 4–7). The analysis of

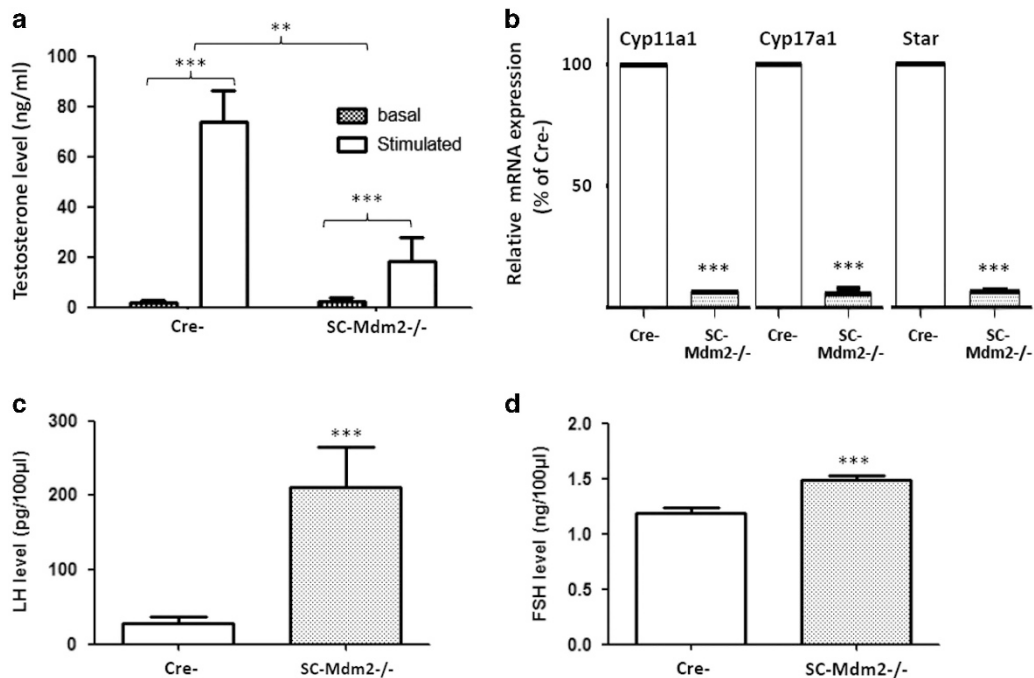


Figure 3 SC-Mdm2^{-/-} hormonal status. (a) Plasma testosterone levels in adult SC-Mdm2^{-/-} males, in basal conditions and after human chorionic gonadotropin (hCG) stimulation. In both SC-Mdm2^{-/-} and Cre- (8 males for each genotype), hCG induced a significant increase (****P*<0.001) in testosterone secretion, as expected. Plasma testosterone levels decreased significantly in SC-Mdm2^{-/-} compared with Cre- (***P*<0.01). Data shown as mean ± S.E.M.; statistical analyses: two-way ANOVA followed by Bonferroni's *post hoc* test; hatching: basal levels; white: hCG stimulated levels. (b) SC-Mdm2^{-/-} testes exhibit a decrease in mRNA levels of Cyp17a1 (P450c17), Cyp11a1 (P450scc) and Star. The amounts of mRNA of the three steroidogenic genes were compared between SC-Mdm2^{-/-} and Cre- (*n*=5 mice for each genotype, tested in triplicate) using TaqMan quantitative real-time PCR as described in Materials and Methods. Normalization was performed with two housekeeping genes, β -actin and GAPDH, that both exhibited similar expression between samples. Results are presented as % of mRNA level in Cre- (100 is arbitrary level for whole Cre- testes) and a non-parametric test (Mann-Whitney) was chosen for the statistical analysis (****P*<0.001). White: Cre-; hatching: SC-Mdm2^{-/-}. (c) LH levels in SC-Mdm2^{-/-} males: plasma LH concentrations expressed in pg/100 μ l in Cre- (*n*=13) and SC-Mdm2^{-/-} (*n*=19) determined by RIA. (d) FSH levels in SC-Mdm2^{-/-} males: plasma FSH concentrations expressed in ng/100 μ l in Cre- (*n*=16) and SC-Mdm2^{-/-} (*n*=23) determined by RIA. Data shown as mean ± S.E.M. Statistical analysis: Mann-Whitney test (****P*<0.001). White: Cre-; hatching: SC-Mdm2^{-/-}

sections at P1 already indicated a pronounced reduction in gonad size ($0.10 \mu\text{l}^{**} \pm 0.01$ versus $0.38 \mu\text{l} \pm 0.02 \mu\text{l}$, *n*=4, *P*<0.01, respectively, for SC-Mdm2^{-/-} and the control) with an almost total loss of cord structures. Testicular cord disappearance was similarly pronounced at E18, while a few cords could still be retrieved at E16 and E15. To understand this phenomenon, apoptosis was investigated by observing TUNEL (Figures 4 and 5) and cleaved-caspase 3 (Figure 6). Both methods similarly revealed numerous apoptotic cells in the SC-Mdm2^{-/-} testes at all the stages examined (e.g., 29 ± 11 versus 150 ± 22 cells/mm², *n*=4, respectively, for the control and SC-Mdm2^{-/-} at P1). Interestingly, double AMH-TUNEL staining clearly indicated that dying cells were mostly SCs at E15 and E16 (Figure 4). Quantification of AMH-TUNEL cells evidenced a significantly increased apoptosis (1.2 ± 0.7 versus $37.2 \pm 2.7\%$, *n*=3–5, respectively, for the control and SC-Mdm2^{-/-} at E15). Of interest, we observed no evidence for senescence based on the absence of p21 or heterochromatin foci in these cells (data not shown). As Mdm2 invalidation is expected to activate p53, double AMH-p53 staining was performed at E15. In control testes (Cre-), hardly any AMH-positive cells expressed detectable levels of p53, whereas in SC-Mdm2^{-/-} testes, we observed that many AMH-positive cells were clearly stained for p53 (Figure 5).

To clarify the identity and fate of the cells remaining in the absence of SCs, germ cell and Leydig cell populations were analyzed in developing SC-Mdm2^{-/-} testes. Germ cells were identified using DDX4 staining (Figure 6) at E15 and P1. As expected, they aggregated in the cords in the control testes. A similar gathering of germ cells (despite the absence of cords or lack of SCs) was retrieved in E15 and E16 testes in SC-Mdm2^{-/-} testes; subsequently, germ cells tended to be more dispersed throughout the testis (E18 and P1). Surprisingly, we could still observe many DDX4-positive cells in P1 testes, indicating that the loss of the supporting SCs did not immediately trigger germ cell death. As SCs are believed to produce a meiosis-repressing environment for germ cells during fetal life, we analyzed the possible presence of the meiotic marker, SYCP3 (Figure 6). In control testes, SYCP3-positive cells were virtually absent, whereas in SC-Mdm2^{-/-} testes, we detected numerous SYCP3-positive cells, all equally positively stained for DDX4. A close examination of the localization of SYCP3 using immunofluorescence (Figures 6i and j) indicated that SYCP3 formed fine threads in the germ cell nuclei, probably along the chromosomal axis, as expected in meiotic cells. Leydig cells were detected using 3 β HSD staining (Figure 7). As expected, they were retrieved between the cords in the control testes and formed well-organized clusters around birth. In SC-Mdm2^{-/-}

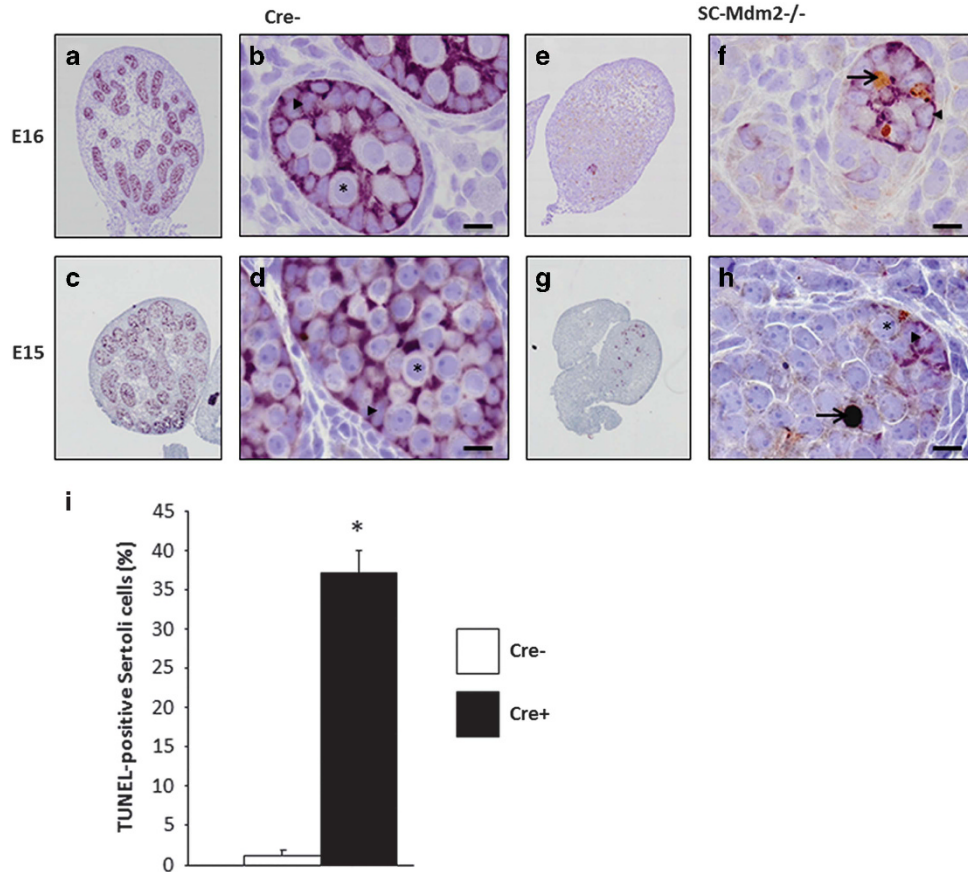


Figure 4 Loss of testicular cords during development is associated with SC apoptosis. Double AMH (purple)/TUNEL (brown) staining was performed with testes at E15 and E16 from control (Cre- **a-d**) and SC-Mdm2^{-/-} (**e-h**) embryos. Left panels (**a, c, e, g**: low magnification) represent an overview of a representative section of the testes (cartography). Right panels (**b, d, f, h**: high magnification) represent testicular cords at high magnification. AMH and TUNEL staining were used to reveal apoptotic SCs. A normal cord-like structure was observed in the control testes with SCs surrounding gonocytes. A pronounced loss of AMH staining was observed in SC-Mdm2^{-/-} and the few remaining AMH-positive cells were frequently positive for TUNEL staining as well, indicating that apoptosis occurred mainly in SCs at these stages. Arrowheads point to healthy SCs (**b, d** and **f, h**), arrows point to apoptotic SCs (**f, h**: double purple/brown positive) and asterisks indicate germ cells or gonocytes. Bars represent 10 μ m. (i) Measurement of SC apoptosis. The percentage of cells positive for both AMH and TUNEL out of total AMH-positive cells was determined at E15 in Cre- ($n=3$) and SC-Mdm2^{-/-} ($n=5$) testis. Data shown as mean \pm S.E.M. Statistical analysis: Mann-Whitney test (* $P<0.05$)

testes, the density of Leydig cells was normal. However, they did not form tight clusters. Interestingly, these cells were still retrieved in adult mutant testes that appeared literally packed with 3 β HSD-positive cells. This clearly indicated that the presence of SCs was dispensable for Leydig cell maintenance in this model.

To verify the implication of the *p53* tumor suppressor gene in the phenotype, we created a new line by introgressing the SC *Mdm2* inactivation in the *p53*^{-/-} line, as described in Materials and Methods (*p53*^{-/-} being normally fertile). Mating was conducted until at least four individuals of each genotype of interest and their respective controls were obtained (Table 1). As expected, SC-Mdm2^{-/-}*p53*^{+/+} were infertile with the same phenotype as SC-Mdm2^{-/-}, whereas their controls Cre-*p53*^{+/+} were fertile. Conversely, SC-Mdm2^{-/-} lacking *p53* (SC-Mdm2^{-/-}*p53*^{-/-}) were normally fertile proving that the phenotype due to *Mdm2* inactivation involves *p53*. One *p53* allele (SC-Mdm2^{-/-}*p53*^{+/-}) is sufficient to maintain the infertility phenotype.

Discussion

To date, few studies have examined the critical factor for SC survival and the development of a gonad devoid of SCs. We report here that *Mdm2* is critical to prevent SC apoptosis and that its specific inactivation triggers a rapid loss of this lineage in testes. Without SCs, Leydig cells persisted, albeit with reduced steroidogenic activity and germ cells did not differentiate properly and only survived a few days.

Mdm2 is a key regulator of *p53*-mediated apoptosis and is proven to be a major downregulator of *p53* in many cell types such as kidney cells,¹⁸ cardiomyocytes,¹⁹ neuronal cells,²⁰ smooth muscle cells²¹ and hepatocytes.²² In testes, the role of *Mdm2* has already been documented in germ cells. *Mdm2* is one mechanism leading to *p53* inactivation in male GCs.²³ It is also suggested that *p53* mediates spermatogonial apoptosis after DNA damage²⁴ or overheating.²⁵ Contrary to GCs, SC apoptosis is poorly documented as it is suspected that this phenomenon is rare. *p53* was suggested to be involved in an intrinsic apoptotic program in SCs, but poorly active.⁵

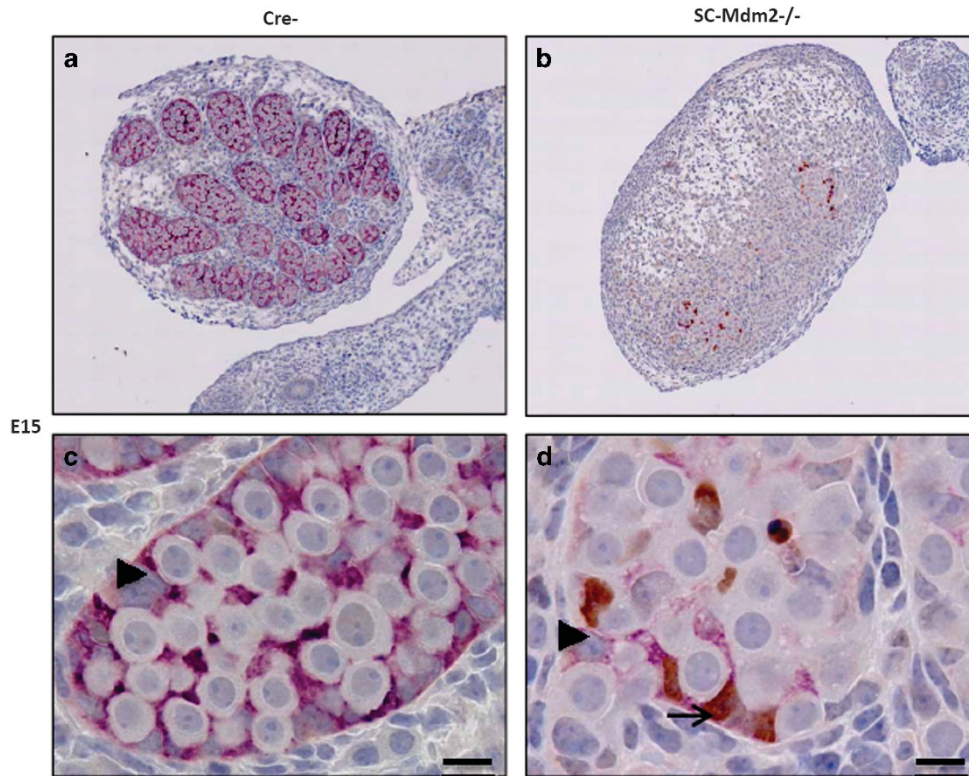


Figure 5 SC apoptosis is correlated with p53 activation. The activation of P53 was investigated in SCs at E15 in control (Cre-) (a, c) and SC*Mdm2*^{-/-} (b, d) testes through double p53/AMH immunostaining. Upper panel represents a global view of a testis section and lower panel a higher magnification of testicular cords. No p53 was observed in control SCs (a, c), while many p53-positive cells (brown) were detected in cord-like structures in SC*Mdm2*^{-/-} (b, d). Interestingly, most were clearly positive for AMH staining (purple) as well. Arrowheads point to p53-negative SCs (c and d) and arrows point to p53-positive SCs (d: double positive). Bars represent 10 μ m

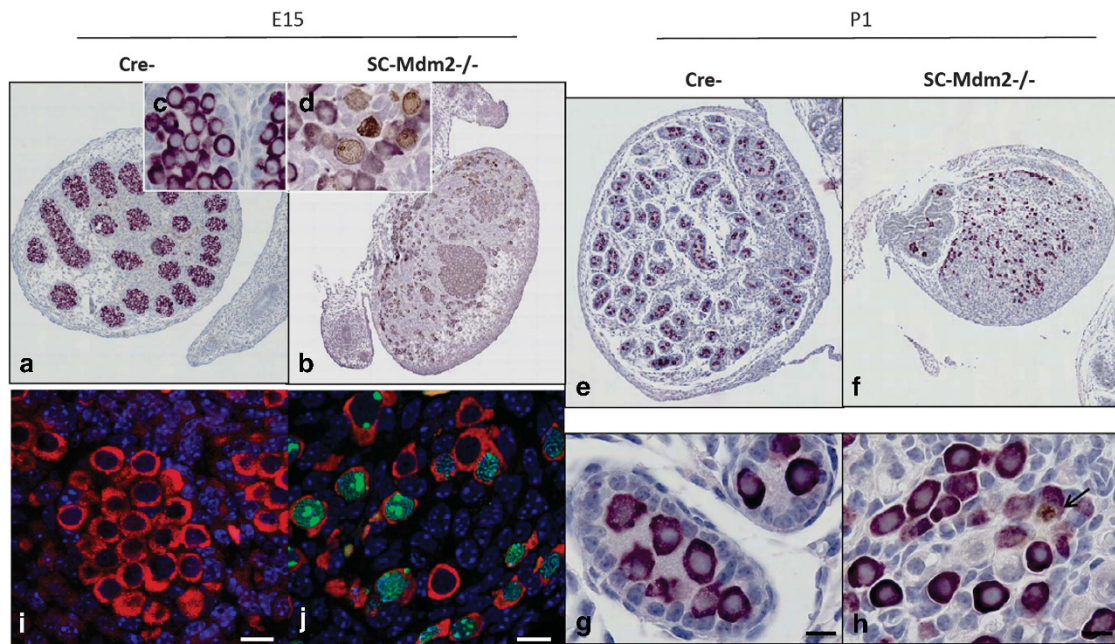


Figure 6 Maintenance of germ cells and premature meiotic entry in absence of SC. DDX4 was investigated by immunostaining (purple) or immunofluorescence (red) in E15 (a-d, i, j) and P1 (e-h) testes from control (Cre-) and SC*Mdm2*^{-/-} animals to follow the germ cell population. DDX4/SYCP3 double immunostaining was performed in E15 testes: immunohistochemistry (a-d: purple for DDX4 / brown for SYCP3; c, d insets provide a higher magnification of germ cells), and immunofluorescence (i, j: DDX4 in red, SYCP3 in green forming obvious filaments in germ cell nuclei) indicated that no SYCP3-positive cells were present in the control testes, while many were retrieved in the SC*Mdm2*^{-/-} testes. Double DDX4 (purple)/cleaved caspase3 (brown) immunostaining was performed in P1 testes. Upper panels (e, f) represent a global view of a testis section and lower panels a higher magnification (g, h). In both control and SC*Mdm2*^{-/-} testes, numerous germ cells and few apoptotic cells were retrieved (i.e., positive for caspase 3: in H7, the arrow points to an apoptotic germ cell). Bars represent 10 μ m

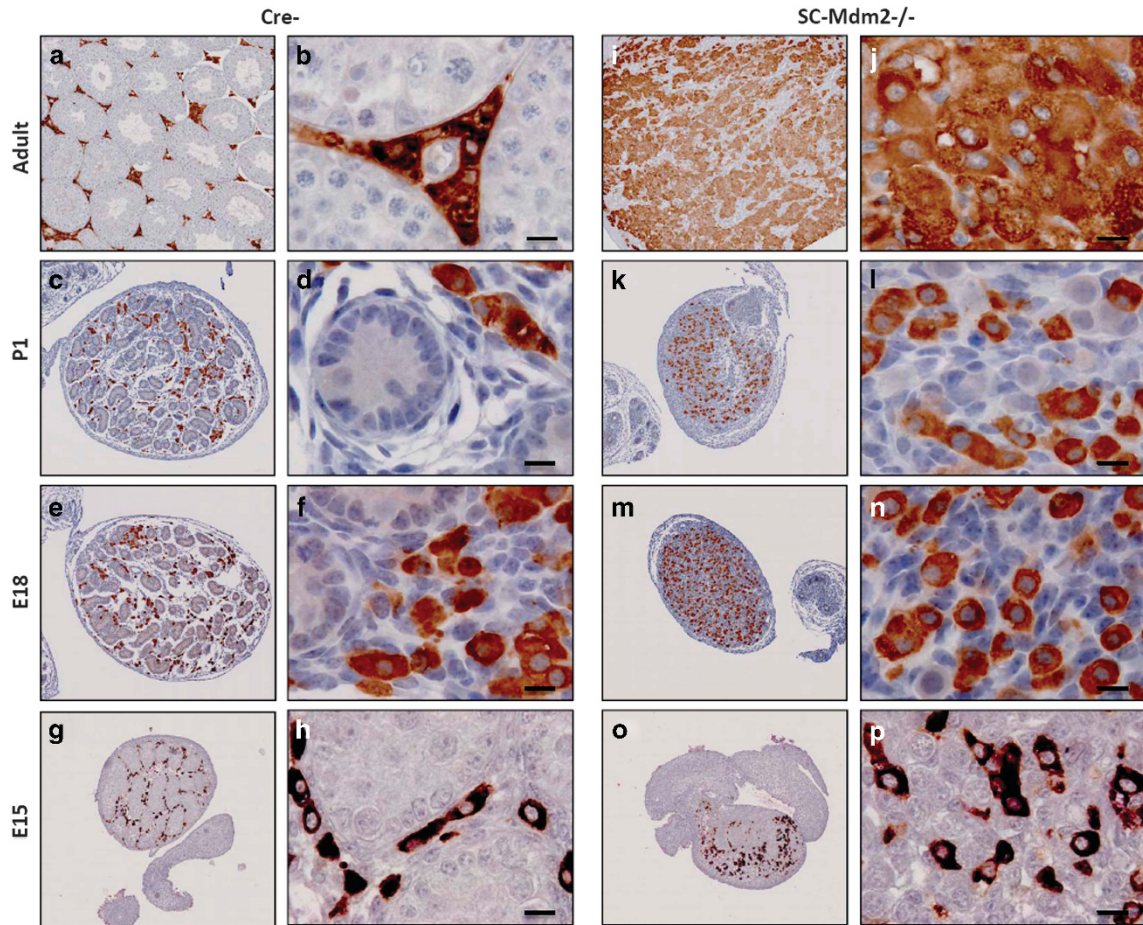


Figure 7 Maintenance of Leydig cells in absence of SCs. 3 β HSD staining (brown) in E15, E18, P1 and adult controls (Cre-) (a to h) and SC-Mdm2^{-/-} (i to p) testes detected Leydig cells. Left panels (low magnification: a, c, e, g for Cre- and i, k, m, o for SC-Mdm2^{-/-}) represent an overview of a representative section of the testes (cartography). Right panels represent high magnifications (b, d, f, h for Cre- and i, k, m, o for SC-Mdm2^{-/-}). Numerous Leydig cells were retrieved in both genotypes at all ages studied. Bars represent 10 μ m

Table 1 Individual male number (#) and fertility status tested with 2 or 4 normal females (f), of the three genotypes corresponding to the introgression of SC-Mdm2^{-/-} in p53: SC-Mdm2^{-/-}p53^[-/- or +/- or +/+], and their corresponding controls: Cre- p53^[-/- or +/- or +/+]

SC-Mdm2^{-/-}p53^{-/-}		Cre- p53^{-/-}	
#3638	fertile (2f)	#3629	fertile (2f)
#3630	fertile (2f)	#3631	fertile (2f)
#3634	fertile (2f)	#3632	fertile (2f)
#3881	fertile (2f)	#3879	fertile (2f)
SC-Mdm2^{-/-}p53^{+/-}		Cre- p53^{+/-}	
#3880	sterile (4f)	#3990	fertile (2f)
#4248	sterile (4f)	#3991	fertile (2f)
#3989	sterile (4f)	#3988	fertile (2f)
#4933	sterile (4f)	#3633	fertile (2f)
SC-Mdm2^{-/-}p53^{+/+}		Cre- p53^{+/+}	
#3992	sterile (4f)	#4934	fertile (2f)
#4245	sterile (4f)	#4246	fertile (2f)
#4783	sterile (4f)	#4247	fertile (2f)
#4935	sterile (4f)	#0922	fertile (2f)

Males are contemporary

Nevertheless, the role of *Mdm2* in SCs had not been examined prior to this work. The inactivation of *Mdm2* using AMH-Cre led to a rapid increase in the p53 protein and apoptotic markers triggering an almost total loss of SCs during fetal life.

As expected, this phenotype was alleviated when p53 was inactivated in the p53^{-/-} genetic background. This demonstrates that p53 activity is strongly repressed in fetal SCs, and may explain the relative poor radiosensitivity of this cell type.²⁶ As p53 is expressed in various testicular cells (and not only SCs), we cannot exclude the p53 effect in other testicular cell types leading to SC apoptosis. Targeted deletion in SCs (using p53^{loxP/loxP27}) would allow to reach this point.

Fetal SCs are critical for the masculinization of the embryo, both indirectly through androgen production by LC and directly as they produce AMH, the hormone inducing the regression of the female genitalia. We report here that SC-Mdm2^{-/-} males displayed a pronounced decrease in AMH staining as early as E15. The extra duct persisting at adulthood in those mice is probably due to this drop. This lack of female duct regression has been observed previously in AMHR2KO and AMHKO males.^{28,29}

SCs are essential for the differentiation of fetal Leydig cells.³⁰ Of interest, we report here that even in the absence of SCs and testicular cords, LC were observed in adult testes. This suggests that SCs are dispensable for the increase and maintenance of the LC population during late fetal and post-natal life. Future work will definitively need to address the nature of the numerous steroidogenic cells observed in

SC-Mdm2^{-/-}. It is also noticeable that SC-Mdm2^{-/-} adult testes produced low levels of androgens, according to the testosterone assay and the measurement of the expression of steroidogenic enzymes. This decrease in testosterone production also probably occurred perinatally, as a decrease in ano-genital distance was observed in SC-Mdm2^{-/-} males. Although ano-genital distance was recently reported to conserve some degree of plasticity at adulthood,³¹ most of it is determined by testosterone production during late fetal life. Altogether, this proves that the presence of SCs is critical for sustaining LC activity and the production of androgens during both fetal and post-natal life. Some androgens were probably produced during the development of SC-Mdm2^{-/-} males, as the male genitalia were formed properly (e.g., presence of epididymis), and testicular descent, which is partially dependent upon androgens, occurred correctly. Testes are indeed formed in the abdominal cavity during fetal life and descend to reach a scrotal position in post-natal life. This depends on the production of two main LC hormones: first, INSL3, a peptide involved in the initial steps of the descent, and second, testosterone.³² We observed no cryptorchidism in SC-Mdm2^{-/-} males, which proves that enough testosterone and INSL3 were produced during fetal life. Thus, this secretion of LC is probably not dependent upon SC regulation.

Quite surprisingly, we observed that the loss of SCs did not trigger an immediate extinction of the germ lineage. In SC-Mdm2^{-/-}, numerous germ cells were retrieved in neonatal testes several days after SC loss. However, germ cells were completely lost at adulthood confirming the absolute requirement of a supporting lineage for the long-term maintenance of germ cells. Fetal SCs are known to govern the orientation toward the male fate of germ cells through the production of Fgf9 and Cyp26b1, and thus to prevent meiotic entry during fetal life.³³ In this context, our report of a premature meiotic entry is not surprising. However, the sex of germ cells is determined between E12 and E14, so one would not expect meiotic entry owing to a late loss of SCs (i.e., at E15). We may thus consider that SCs are required both to impose and to maintain a male fate in germ cells. In addition, the seemingly proper differentiation of LC and the altered one of germ cells fits well with fetal LC differentiation occurring prior to germ cell differentiation (i.e., determination of fate during fetal life).

Very recently, another study successfully produced SC-deficient testes.^{34,35} This work used the diphtheria toxin expressed by SCs and the same AMH-Cre system as in our work. Our SC-Mdm2^{-/-} model proposed here is complementary as it precludes the risk related to using a toxin with possible side effects. Moreover, Rebouret and colleagues indicate a variable phenotype with, in most cases (95%), a mere 60% reduction in the size of adult testes, possibly owing to a partial ablation of SCs in response to expression of the toxin. The invalidation of *Mdm2* thus offers a more efficient and reproducible ablation of SCs, as we systematically obtained (around 30 males examined for the entire study) a 95% reduction in testis weight. The overall conclusions of both studies converge toward SCs being required to sustain germ and Leydig cell activity with a total loss of germ cells and the presence of a population of LC in adult testes. A slight difference related to the masculinization (e.g., differentiation of epididymis and vas deferens owing to testosterone

production) was observed that did not seem to occur following expression of the toxin, whereas it is obvious following *Mdm2* invalidation. We believe this may be due to the partial loss of SCs in the former system. Finally, these authors also reported the persistence of SOX9-positive cells in the rete area, as observed here, due to epithelial cells in the rete only partially expressing Cre.

As a whole, our work provides a clear demonstration of the crucial role of *Mdm2*/p53 in the regulation of SC apoptosis and opens new possibilities for studying the role of this cell type, thanks to efficient ablation during fetal life. Future works will need to characterize the precise kinetics of dysfunctions in LC in the absence of SCs.

Materials and Methods

Animals. Mice were fed a standard laboratory diet and tap water *ad libitum*, and maintained under 12L:12D photoperiods in a temperature-controlled room (21–23 °C). All animal studies were conducted in accordance with the guidelines for the care and use of laboratory animals issued by the French Ministry of Agriculture and with the approval of a local ethical committee (number 2011-12-3, Comité d'Ethique en Expérimentation Animale Val de Loire – n°19). All efforts were made to minimize animal stress and suffering.

Generation of SC-Mdm2^{-/-} and SC-Mdm2^{-/-}p53^{-/-} and their respective controls. *Mdm2*^{2L} mice were previously described by Grier *et al.*³⁶ and contain a floxed *Mdm2* allele with a loxP site in intron 4, followed by a neomycin cassette, and a second loxP site in intron 6. Recombination yields an *Mdm2* allele lacking exons 5 and 6 (*Mdm2*[δ exons5/6]) after the Cre recombination event, resulting in a loss of most of the p53-binding domain.³⁶ *Mdm2*^{2L} were crossed with heterozygous AMH-Cre mice on a C57BL/6 background, and the resulting Cre + *Mdm2*^{-/+} offspring were backcrossed to *Mdm2*^{2L} mice to obtain Cre + *Mdm2*^{-/-}, so called SC-Mdm2^{-/-}; controls were contemporary Cre-*Mdm2*^{2L} littermates, called Cre- here for simplicity.

p53^{-/-} (null) mice were obtained from the Jackson laboratory (Sacramento, CA, USA) and were normally fertile. Cre + *Mdm2*^{-/-} females were bred with p53^{-/-} males, and the resulting Cre + *Mdm2*^{-/-} p53^{-/-} offspring were intercrossed to obtain homozygous mice for invalid *Mdm2* alleles (*Mdm2*^{-/-}), followed by intercrossing to obtain males with key genotypes: SC-Mdm2^{-/-}p53^{+/+}; SC-Mdm2^{-/-}p53^{-/-}; SC-Mdm2^{-/-}p53^{+/-}; and their respective contemporary littermate controls: Cre-p53^{+/-}; Cre-p53^{-/-}; Cre-p53^{+/+}.

A high predisposition to malignancy was described for homozygous p53^{-/-}, with a greatly accelerated rate of tumorigenesis.³⁷ To avoid the risk of cancer, we used these mice for breeding and experiments before the age of 3.5 months.

Male fertility test. For each genotype of interest (SC-Mdm2^{-/-}, SC-Mdm2^{-/-}p53^{+/-}, SC-Mdm2^{-/-}p53^{-/-}, SC-Mdm2^{-/-}p53^{+/+} and heterozygous SC-Mdm2^{-/+}), each adult male (at least four per genotype) was mated with two or four primiparous Swiss female mice.

Mouse genotyping. PCR genotyping of Cre, *Mdm2* and p53 alleles have been described previously (Lécureuil *et al.*,¹⁷ Montes *et al.*¹⁵ and Jones *et al.*,¹⁶ respectively). DNA was extracted using the Tissue PCR Kit (Sigma-Aldrich, Saint Quentin Fallavier, France). GABR detection (200 bp) was used to control DNA quality.

To verify that excision was restricted to the testes, DNA was extracted from various tissues, including testes from prepubertal mice, and PCR was performed using primers previously described³⁶ to detect the deleted allele lacking exons 5 and 6 (*Mdm2*[δ exons5/6]): forward: 5'-TGTGGAGAAACAGTTACTTC-3'; reverse 5'-TGAGATGAGTCAAAGCCTGG-3'. The annealing temperature was 50 °C.

Gene expression analysis

RNA extraction. Total RNA was isolated from whole testes (adult or P10) and from SC-enriched fractions obtained at P10 and prepared as described previously³⁸ using RNAsol reagent (Eurobio, Courtaboeuf, France). RNA (1 μ g) was reverse-transcribed using the RNeasy kit (QIAGEN, Courtaboeuf, France) according to the manufacturer's instructions (the kit includes genomic DNA elimination with DNase). The sample with RNA but without RT (RT-) was the negative control.

RT-PCR for *Mdm2* mRNA detection: Classic PCR was performed with Taq polymerase from Eurobio to detect *Mdm2* mRNA in SC-enriched fractions. *Mdm2* mRNA-specific primers (band at 180 bp), described in a previous study³⁹ were: forward 5'-CGGAAGARGCGCGAAAGTA-3'; reverse 5'-TTCGGAAGCTGGAARCTGTGAGGTGC-3'. The annealing temperature was 60 °C. For actin detection (band at 411 bp), used to control DNA quality, the primers were: forward: 5' TAC GAC CAG AGG CAT ACA GG 3' reverse: 5' TGA CCC AGA TCA TGT TTG AGA 3'. The annealing temperature was 55 °C.

Quantitative real-time PCR analysis for the investigation of testicular steroidogenesis: Three steroidogenic genes were analyzed using the TaqMan assay, with primers and probes inventoried by Applied Biosystems (Fisher Scientific, Illkirch, France): StAR (Steroidogenic acute regulatory protein, Mm00441558_m1); P450scc -Cyp11a1- (cytochrome P450 side-chain cleavage enzyme, Mm00490735_m1); P450c17 -Cyp17a1- (steroid 17 α hydroxylase/17,20 lyase cytochrome P450c17, Mm00484040_m1). PCR reagents were all purchased from Applied Biosystems (Fisher Scientific) and real-time PCR was carried out in accordance with the manufacturer's instructions in a final volume of 25 μ l (samples were run in triplicate). Fluorescence was detected on an iCycler Bio-Rad apparatus (Bio-Rad, Marnes la Coquette, France). Negative controls (RT – and H₂O) were run for every primer/probe combination. Normalization was performed using two internal standards, β -actin (Mm00607939_s1) and Gapdh (Mm99999915_g1) from the same sample, and the normalized cDNA was compared between the two genotypes.

Blood collection and hormonal assay. Around 500 μ l of blood were obtained by retro-orbital sampling in anesthetized mice (with diazepam and ketamine), and collected in a tube containing EDTA.

Plasma testosterone levels: Mice were treated with an intraperitoneal injection of 15 IU per animal of human chorionic gonadotropin (Chorulon, MSD Santé Animale, Beaucouze, France). Blood was collected before (basal level) and 2 h after injection (stimulated level). The plasma was stored at –20 °C until tritium-based testosterone competitive radio-immunoassays, which are carried out regularly in our lab, were performed in our lab as described previously for other transgenic lines.⁴⁰ The sensitivity of the assay was 0.125 ng/ml and the intraassay coefficient of variation was 7.5%. Briefly, samples (two dilutions per sample) or testosterone dilutions (to determine the range) were incubated for 1 h at 40 °C (0.1 M phosphate buffer with 0.1% gelatin) with tritiated testosterone plus the anti-testosterone antibody. A secondary antibody was then added and the mixtures incubated overnight at 4 °C. Immuno-precipitation was then performed with PEG (PolyEthyleneGlycol) 4000 and the radioactivity counted (Packard C2900, TriCarb, PerkinElmer, Villebon S/Yvette, France).

Plasma FSH levels: Plasma FSH levels were determined in 100 μ l aliquots using a double Ab method and a RIA kit (rFSH RIA), kindly supplied by the National Institutes of Health (Dr A. F. Parlow, National Hormone and Peptide Program, Torrance, CA, USA). Rat FSH antigen (NIDDK-rFSH-I) was labeled with ¹²⁵I using the chloramine-T method and the hormone concentration was expressed using the rat FSH reference preparation (NIDDK-rFSH-RP-2) as the standard. Intraassay and interassay coefficients were less than 7% and 10%, respectively. The sensitivity of the assay was 0.125 ng/100 μ l.

Plasma LH levels: Plasma LH levels were determined in 100 μ l aliquots using a double Ab method and a RIA kit (mLHRia), kindly supplied by the National Institutes of Health (Dr A. F. Parlow, National Institute of Diabetes and Digestive and Kidney Diseases, National Hormone and Peptide Program). Rat LH-I-10 (AFP-11536B) was labeled with ¹²⁵I using the chloramine-T method and the hormone concentration was expressed using the mouse LH reference preparation (AFP-5306 A) as the standard. Intraassay and interassay coefficients were less than 7% and 10%, respectively. The sensitivity of the assay was 4 pg/100 μ l.

Histology and immuno-detection of AMH, DDX4, 3 β HSD, C-CASPASE3, SYCP3 and p53. Testis histology (seminiferous tubule organization) was analyzed after fixing in Bouin's fluid and embedding in paraffin. For microscopic observation, 4- μ m sections were stained with hematoxylin.

Immunostaining was performed as described previously⁴¹ with minor modifications. Fetal, postnatal and adult testes were fixed overnight in 10% neutral formalin (Carlo Erba Reagents, Val de Reuil, France) before being dehydrated, embedded in paraffin wax and cut into 5- μ m sections. Adult testes were stained with hematoxylin and eosin; fetal and postnatal testes were used for immunostaining. The primary antibodies used in this study were either rabbit polyclonal anti-DEAD/H box polypeptide 4 (DDX4/VASA; 1 : 200, Abcam, Paris, France), rabbit polyclonal anti-

cleaved caspase-3 (1 : 200, Cell Signaling/Ozyme, Montigny-Le-Bretonneux, France), goat polyclonal anti-AMH (1 : 200, Santa Cruz Biotechnology, Heidelberg, Germany), mouse monoclonal anti-3 β HSD (1 : 200, Transgenic Inc., Chuo-Ku, Kobe, Japan), mouse monoclonal anti-SYCP3 (Abcam 1/200), mouse monoclonal anti-P21 (1 : 200, BD Biosciences, le Pont de Claix, France) or rabbit polyclonal anti-TP53 (1/500, Novocastra, Leica Microsystems, Nanterre, France). The same protocol was used for antigen retrieval. After testis section dewaxing and rehydration, antigen retrieval was performed in HIER citrate buffer pH 6 (Zytomed, Diagomics, Blagnac, France) in an autoclave (Retriever 2100, Proteogenix, Mundolsheim, France). Sections were then washed in distilled water and incubated for 15 min in 3% H₂O₂ at room temperature. After 30 min in 2.5% normal Horse serum (Vector laboratories, Eurobio, Les Ulis, France), primary antibodies diluted in PBS were incubated for 1 h at 37 °C. Primary antibodies were revealed using the secondary antibody IMPRESS kit (Vector Laboratories, Eurobio). Peroxidase activity was visualized using either 3,3'-diaminobenzidine (brown) or vip (purple) as a substrate. Sections were counterstained with hematoxylin. TUNEL staining was performed using the Apoptag peroxidase kit (MP Biomedicals, Illkirch, France) in accordance with the manufacturer's recommendations. For cell counting, at least 300 cells were counted in three different sections for each testis. For immunofluorescence detection, primary antibodies were detected with specific secondary antibody species Alexa Fluor 488- and Alexa Fluor 594-conjugated antibodies (1 : 500, Life Technologies, Saint Aubin, France).

Statistical analysis. All data are presented as means \pm S.E.M. To compare means between two groups, the Student's *t* test or the Mann-Whitney *U* test, in case of differences in variance (Fisher test), was used. Other comparisons were performed using a two-way ANOVA followed by the Bonferroni post-test. *P* < 0.05 was considered significant.

Conflict of Interest

The authors declare no conflict of interest.

Acknowledgements. We would like to thank Claude Cahier and Deborah Crespin for the animal facilities. Special thanks go to Christophe Gauthier for the testosterone assays, Isabelle Gibert, Peggy Jarrier and Linda Beauclair for the genotyping, Mrs Arlette Gerard for the FSH and LH assays and Marie Françoise Pinault for her help managing the pictures. Florian Guillou is thanked for providing AMH-Cre line. The English was proofread and corrected by Helen Lamprell from HSB Traductions. This work was funded by two grants from the Agence Nationale pour la Recherche ('Biodiversité, évolution des écosystèmes, écosystèmes productifs, agronomie' grant; 2011-2013): TimeOfLife2 and EarlyFol.

1. Svingen T, Koopman P. Building the mammalian testis: origins, differentiation, and assembly of the component cell populations. *Genes Dev* 2013; **27**: 2409–2426.
2. Svechnikov K, Landreh L, Weisser J, Izzo G, Colón E, Svechnikova I et al. Origin, development and regulation of human Leydig cells. *Horm Res Paediatr* 2010; **73**: 93–101.
3. Lejeune H, Chuzel F, Thomas T, Avallet O, Habert R, Durand P et al. Paracrine regulation of Leydig cells. *Ann Endocrinol* 1996; **57**: 55–63.
4. Moreno SG, Dutrillaux B, Coffigny H. High sensitivity of rat foetal germ cells to low dose-rate irradiation. *Int J Radiat Biol* 2001; **77**: 529–538.
5. Lambrot R, Coffigny H, Pairault C, Lécureuil C, Frydman R, Habert R et al. High radiosensitivity of germ cells in human male fetus. *J Clin Endocrinol Metab* 2007; **92**: 2632–2639.
6. Hall PA, Lane DP. Tumor suppressors: a developing role for p53? *Curr Biol* 1997; **7**: R144–R147.
7. Levine AJ, Tomasini R, McKeon FD, Mak TW, Melino G. The p53 family: guardians of maternal reproduction. *Nat Rev Mol Cell Biol* 2011; **12**: 259–265.
8. Cavallo F, Feldman DR, Barchi M. Revisiting DNA damage repair, p53-mediated apoptosis and cisplatin sensitivity in germ cell tumors. *Int J Dev Biol* 2013; **57**: 273–280.
9. Matsui Y, Nagano R, Obinata M. Apoptosis of fetal testicular cells is regulated by both p53-dependent and independent mechanisms. *Mol Reprod Dev* 2000; **55**: 399–405.
10. Beumer TL, Roepers-Gajadien HL, Gademian IS, van Buul PP, Gil-Gomez G, Rutgers DH et al. The role of the tumor suppressor p53 in spermatogenesis. *Cell Death Differ* 1998; **5**: 669–677.
11. Levine AJ. p53, the cellular gatekeeper for growth and division. *Cell* 1997; **88**: 323–331.
12. Prives C, Hall PA. The p53 pathway. *J Pathol* 1999; **187**: 112–126.
13. Lavin MF, Gueven N. The complexity of p53 stabilization and activation. *Cell Death Differ* 2006; **13**: 941–950.

14. Marine JC, Lozano G. Mdm2-mediated ubiquitylation: p53 and beyond. *Cell Death Differ* 2010; **17**: 93–102.
15. Montes de Oca Luna R, Wagner DS, Lozano G. Rescue of early embryonic lethality in *mdm2*-deficient mice by deletion of p53. *Nature* 1995; **378**: 203–206.
16. Jones SN, Roe AE, Donehower LA, Bradley A. Rescue of embryonic lethality in *Mdm2*-deficient mice by absence of p53. *Nature* 1995; **378**: 206–208.
17. Lécureuil C, Fontaine I, Crepieux P, Guillou F. Sertoli and granulosa cell-specific Cre recombinase activity in transgenic mice. *Genesis* 2002; **33**: 114–118.
18. Hilliard S, Aboudehen K, Yao X, El-Dahr SS. Tight regulation of p53 activity by *Mdm2* is required for ureteric bud growth and branching. *Dev Biol* 2011; **353**: 354–366.
19. Grier JD, Xiong S, Elizondo-Fraire AC, Parant JM, Lozano G. Tissue-specific differences of p53 inhibition by *Mdm2* and *Mdm4*. *Mol Cell Biol* 2006; **26**: 192–198.
20. Lovell MA, Xie C, Xiong S, Markesbery WR. Wilms' tumor suppressor (WT1) is a mediator of neuronal degeneration associated with the pathogenesis of Alzheimer's disease. *Brain Res* 2003; **983**(1-2): 84–96.
21. Boesten LS, Zadelaar SM, De Clercq S, Francoz S, van Nieuwkoop A, Biessen EA *et al*. *Mdm2*, but not *Mdm4*, protects terminally differentiated smooth muscle cells from p53-mediated caspase-3-independent cell death. *Cell Death Differ* 2006; **13**: 2089–2098.
22. Cao W, Zhang JL, Feng DY, Liu XW, Li Y, Wang LF *et al*. The effect of adenovirus-conjugated NDRG2 on p53-mediated apoptosis of hepatocarcinoma cells through attenuation of nucleotide excision repair capacity. *Biomaterials* 2014; **35**: 993–1003.
23. Schwartz D, Goldfinger N, Rotter V. Expression of p53 protein in spermatogenesis is confined to the tetraploid pachytene primary spermatocytes. *Oncogene* 1993; **8**: 1487–1494.
24. Hasegawa M, Zhang Y, Niibe H, Terry NH, Meistrich ML. Resistance of differentiating spermatogonia to radiation-induced apoptosis and loss in p53-deficient mice. *Radiat Res* 1998; **149**: 263–270.
25. Socher SA, Yin Y, Dewolf WC, Morgentaler A. Temperature-mediated germ cell loss in the testis is associated with altered expression. *J Urol* 1997; **157**: 1986–1989.
26. Vergouwen RP, Huiskamp R, Bas RJ, Roepers-Gajadien HL, Davids JA, de Rooij DG. Radiosensitivity of testicular cells in the fetal mouse. *Radiat Res* 1995; **141**: 66–73.
27. Marino S, Vooijs M, van Der Gulden H, Jonkers J, Berns A. Induction of medulloblastomas in p53-null mutant mice by somatic inactivation of Rb in the external granular layer cells of the cerebellum. *Genes Dev* 2000; **14**: 994–1004.
28. Wu X, Arumugam R, Baker SP, Lee MM. Pubertal and adult Leydig cell function in Mullerian inhibiting substance-deficient mice. *Endocrinology* 2005; **146**: 589–595.
29. Mishina Y, Rey R, Finegold MJ, Matzuk MM, Josso N, Cate RL *et al*. Genetic analysis of the Müllerian-inhibiting substance signal transduction pathway in mammalian sexual differentiation. *Genes Dev* 1996; **10**: 2577–2587.
30. Yao HH, Whoriskey W, Capel B. Desert Hedgehog/Patched 1 signaling specifies fetal Leydig cell fate in testis organogenesis. *Genes Dev* 2002; **16**: 1433–1440.
31. Mitchell RT, Mungall W, McKinnell C, Sharpe RM, Cruickshanks L, Milne L *et al*. Anogenital distance (AGD) plasticity in adulthood: Implications for its use as a biomarker of fetal androgen action. *Endocrinology* 2015; **156**: 24–31.
32. Bay K, Main KM, Toppari J, Skakkebaek NE. Testicular descent: INSL3, testosterone, genes and the intrauterine milieu. *Nat Rev Urol* 2011; **8**: 187–196.
33. Bowles J, Feng CW, Spiller C, Davidson TL, Jackson A, Koopman P. FGF9 suppresses meiosis and promotes male germ cell fate in mice. *Dev Cell* 2010; **19**: 440–449.
34. Rebourcet D, O'Shaughnessy PJ, Pitetti JL, Monteiro A, O'Hara L, Milne L *et al*. Sertoli cells control peritubular myoid cell fate and support adult Leydig cell development in the prepubertal testis. *Development* 2014; **141**: 2139–2149.
35. Rebourcet D, O'Shaughnessy PJ, Monteiro A, Milne L, Cruickshanks L, Jeffrey N *et al*. Sertoli cells maintain Leydig cell number and peritubular myoid cell activity in the adult mouse testis. *PLoS One* 2014; **9**: e105687.
36. Grier JD, Yan W, Lozano G. Conditional allele of *mdm2* which encodes a p53 inhibitor. *Genesis* 2002; **32**: 145–147.
37. Jacks T, Remington L, Williams BO, Schmitt EM, Halachmi S, Bronson RT *et al*. Tumor spectrum analysis in p53-mutant mice. *Curr Biol* 1994; **4**: 1–7.
38. Lécureuil C, Saleh MC, Fontaine I, Baron B, Zakin MM, Guillou F. Transgenic mice as a model to study the regulation of human transferrin expression in Sertoli cells. *Hum Reprod* 2004; **19**: 1300–1307.
39. Montes de Oca Luna RM, Tabor AD, Eberspaecher H, Hulboy DL, Worth LL, Colman MS *et al*. The organization and expression of the *mdm2* gene. *Genomics* 1996; **33**: 352–357.
40. Furnel B, Guerquin MJ, Livera G, Staub C, Magistrini M, Gauthier C *et al*. Thyroid hormone limits postnatal Sertoli cell proliferation *in vivo* by activation of its alpha1 isoform receptor (TRalpha1) present in these cells and by regulation of Cdk4/JunD/c-myc mRNA levels in mice. *Biol Reprod* 2012; **87**: 1–9.
41. Livera G, Delbes G, Pairault C, Rouiller-Fabre V, Habert R. Organotypic culture, a powerful model for studying rat and mouse fetal testis development. *Cell Tissue Res* 2006; **324**: 507–21.



This work is licensed under a Creative Commons Attribution-NonCommercial-NoDerivs 4.0 International License. The images or other third party material in this article are included in the article's Creative Commons license, unless indicated otherwise in the credit line; if the material is not included under the Creative Commons license, users will need to obtain permission from the license holder to reproduce the material. To view a copy of this license, visit <http://creativecommons.org/licenses/by-nc-nd/4.0/>

Supplementary Information accompanies this paper on Cell Death and Differentiation website (<http://www.nature.com/cdd>)